# Mitigation of Biodynamic Feedthrough for Touchscreens on the Flight Deck

Khoshnewiszadeh, Arwin; Pool, Daan M.

**DOI**
10.1080/10447318.2021.1890490

**Publication date**
2021

**Document Version**
Final published version

**Published in**
International Journal of Human-Computer Interaction

**Citation (APA)**
Khoshnewiszadeh, A., & Pool, D. M. (2021). Mitigation of Biodynamic Feedthrough for Touchscreens on the Flight Deck. *International Journal of Human-Computer Interaction*, *37*(7), 680-692. https://doi.org/10.1080/10447318.2021.1890490

International Journal of Human–Computer Interaction

ISSN: (Print) (Online) Journal homepage: https://www.tandfonline.com/loi/hihc20

# Mitigation of Biodynamic Feedthrough for Touchscreens on the Flight Deck

Arwin Khoshnewiszadeh & Daan M. Pool

**To cite this article:** Arwin Khoshnewiszadeh & Daan M. Pool (2021) Mitigation of Biodynamic Feedthrough for Touchscreens on the Flight Deck, International Journal of Human–Computer Interaction, 37:7, 680-692, DOI: 10.1080/10447318.2021.1890490

**To link to this article:** https://doi.org/10.1080/10447318.2021.1890490



Published online: 23 Mar 2021.

INTERNATIONAL JOURNAL OF HUMAN–COMPUTER INTERACTION
2021, VOL. 37, NO. 7, 680–692
https://doi.org/10.1080/10447318.2021.1890490



# Mitigation of Biodynamic Feedthrough for Touchscreens on the Flight Deck

Arwin Khoshnewiszadeh and Daan M. Pool

Faculty of Aerospace Engineering, Control & Simulation Section, Delft University of Technology, Delft, The Netherlands

**ABSTRACT**
Biodynamic feedthrough (BDFT) is a key issue for touchscreen operations on the future flight deck, as cockpit accelerations due to turbulence leave pilots vulnerable to erroneous touches that disrupt task performance. This research focuses on the implementation of a software-based cancellation approach to mitigate the adverse effects of BDFT in touchscreen dragging tasks. A flight-simulator experiment with 18 participants was performed to estimate models of BDFT dynamics for horizontal and vertical touch-inputs on a primary flight display. The averaged BDFT models were used to cancel BDFT in the same continuous dragging task used for model identification and a discrete point-to-point dragging task. While for the continuous task the cancellation enabled 63% mitigation in BDFT, the same cancellation was ineffective for the discrete task, due to reduced BDFT susceptibility. Overall, the results show that while model-based BDFT cancellation can be highly effective, a key technical challenge will be ensuring it is sufficiently task-adaptive.

## 1. Introduction

The next evolution of the commercial flight deck will introduce touchscreen devices to replace physical controls, such as buttons and switches. Both Airbus and Boeing have announced touchscreens in the cockpit of their future airliners (Kingsley-Jones, 2018; Trimble, 2016) with Gulfstream's G500/G600 business jets already including ten touchscreen controllers (Watkins et al., 2018). The possible advantages of touchscreens, such as their direct manipulation capabilities, reduction of workload, cost and efficient space usage (Avsar, 2017; Kaminani, 2011), are the main reasons for the current technology push. However, a critical challenge for touchscreen use on the flight deck lies in the well-known problems of operating touch interfaces in vibratory environments (e.g., turbulence), which has shown to increase workload, cause more task errors, and increase fatigue (Cockburn et al., 2017; Dodd et al., 2014).

One key reason for decreased task performance is biodynamic feedthrough (BDFT): the involuntary movement of limbs due to physical accelerations or vibrations (Mobertz et al., 2018; Venrooij, 2014; Venrooij et al., 2013). BDFT causes parts of the body to move in an unintentional manner, which is known to result in *involuntary* and undesired direct feedthrough of perturbed arm/hand movements into touchscreen gesture inputs, as often happens when operating a smart phone while walking. Although BDFT so far has received little attention in regard to touchscreen operation, it has been extensively investigated for other settings where it causes problems, such as input and control tasks with traditional input devices in aircraft and helicopters (Allen et al., 1973; Jex, 1972; Masarati et al., 2015; Mayo, 1989; Venrooij, 2014), hydraulic excavators (Humphreys et al., 2010), and electric wheelchairs (Banerjee et al., 1996). Only a single previous study (Mobertz et al., 2018) has focused on the explicit quantification of BDFT when using a touchscreen in a moving environment. For the effective use of touchscreens on the modern flight deck in all flight conditions, it is essential that an effective approach to the mitigation of BDFT, which can minimize the occurrence of possibly hazardous touchscreen input errors, is developed.

When it comes to BDFT, generally a distinction is made between *closed-loop* BDFT (Sirouspour & Salcudean, 2003; Sövényi & Gillespie, 2007) and *open-loop* BDFT (Venrooij et al., 2010). Closed-loop BDFT occurs if the (combined voluntary and involuntary) control actions of the human controller directly affect the vehicle's movement and thus the accelerations causing BDFT. On the other hand, in open-loop BDFT the control input provided does not influence the perturbing motion accelerations. As on the modern flight deck touchscreen usage is not expected to include direct vehicle control, the mitigation of BDFT for touchscreens in the cockpit is therefore an open-loop BDFT problem (Venrooij et al., 2010).

Several methods have already been proposed for mitigating BDFT, or reducing its effects on task performance. The most direct methods involve the use of different types of hand supports, e.g., high-friction materials or additional grips around the edge of the screens, such as those used in Gulfstream's G500/G600 business jets (Cockburn et al., 2017; Lancaster et al., 2011; Watkins et al., 2018) or elbow supports that can be used to restrict hand movement (Bauersfeld, 1992). Also, it has been proposed to facilitate resting all fingers on the screen while using the index finger only for tapping inputs (Cockburn et al., 2019), or to make use of

**CONTACT** Daan M. Pool d.m.pool@tudelft.nl Faculty of Aerospace Engineering, Control & Simulation Section, Delft University of Technology, P.O. Box 5058, Delft, 2600 GB, The Netherlands

resistive instead of capacitive touchscreens to minimize accidental touch inputs, as proposed by Boeing (Trimble, 2016). For the Airbus A350, Airbus uses a redundancy approach, where a keyboard cursor control unit (KCCU) is considered as a backup in case of turbulence (Airbus, 2019). Finally, also in touchscreen gesture interpretation software steps are taken to avoid wrong selections as much as possible, such as the "land on" and "lift off" methods as implemented on the G500/G600 (Watkins et al., 2018). While these approaches can certainly be useful for tapping and discrete touch inputs, they will not be effective for more continuous *dragging* gestures that will be an integral part of future touchscreen operations on the flight deck (e.g., a waypoint modification) (Alapetite et al., 2012; Gauci et al., 2015; Mertens et al., 2012; Stuyven et al., 2012).

A potentially valuable approach, which has been successfully demonstrated for BDFT with physical control inceptors (Gillespie et al., 1999; Sirouspour & Salcudean, 2003; Sövényi & Gillespie, 2007) is generally referred to as *model-based BDFT cancellation*. This purely software-based approach uses a mathematical model of human BDFT dynamics to predict the involuntary hand movements based on the measured vehicle accelerations. This predicted BDFT is then, in an additional step of software touch input processing, subtracted from the recorded touchscreen input, to mitigate the BDFT component. While a promising approach, as it can straightforwardly be integrated in any touchscreen's input processing software and only requires a measurement of aircraft/cockpit accelerations from inertial sensors as available in most aircraft, a downside of model-based cancellation is that its effectiveness relies directly on the accuracy of the BDFT model (Griffin, 2001; Venrooij et al., 2010).

The goal of this paper is to assess the feasibility of model-based open-loop BDFT cancellation for touchscreens applied to dragging tasks (e.g., waypoint relocation) in turbulence. Specifically, the paper investigates 1) how much of erroneous BDFT-related touchscreen inputs can be canceled with this approach, and 2) the extent to which BDFT models need to be *task dependent* – i.e., adapted to the specific biodynamic properties pilots' have during different input tasks – to be truly effective. This paper describes a dedicated pilot-in-the-loop experiment performed in the SIMONA Research Simulator (SRS) at Delft University of Technology. In the experiment, 18 participants performed two different two-dimensional dragging tasks – i.e., tracking continuous multisine signals or tracking a series of discrete steps – on a touchscreen at the location of the primary flight display. For both tasks, the participants were subjected to motion disturbance signals representative for aircraft turbulence in either their vertical ("heave") or lateral ("sway") axis.

This paper is structured as follows. First, Section 2 will explain the model-based BDFT cancellation. Section 3 describes the human-in-the-loop experiment and analysis methods. The experimental results are presented in Section 4 and discussed in Section 5. The paper ends with the main conclusions.

## 2. BDFT cancellation

BDFT is the involuntary limb movement caused by vibration and is different than voluntary control action, as shown in Figure 1. The voluntary actions come from the central nervous system (CNS), which in order to achieve the goals of the control task applies cognitive commands to the neuromuscular system (Damveld et al., 2013; Venrooij et al., 2010). Although the two can be separated, the voluntary actions do affect the involuntary contributions to the total control input indirectly. For example, by cognitively changing the neuromuscular dynamics, e.g., by tightening or loosening muscles, the susceptibility to BDFT will also change (Mayo, 1989; Venrooij et al., 2011).

In this paper, we consider BDFT for a 2-dimensional touchscreen input task, for which the control input coordinates in lateral-horizontal ($y$) and vertical ($z$) screen coordinates are represented by the control signal $u_{y,z}$, see Figure 1. When performing a certain control task, part of a human pilot's control input $u_{y,z}$ will result from task-related cognitive *voluntary* control action, here indicated as $u^{vol}_{y,z}$. When a task is performed on a moving platform (e.g., vehicle), the motion accelerations and vibrations resulting from the vehicle's motion can cause an additional, involuntary, BDFT component in $u_{y,z}$. In Figure 1

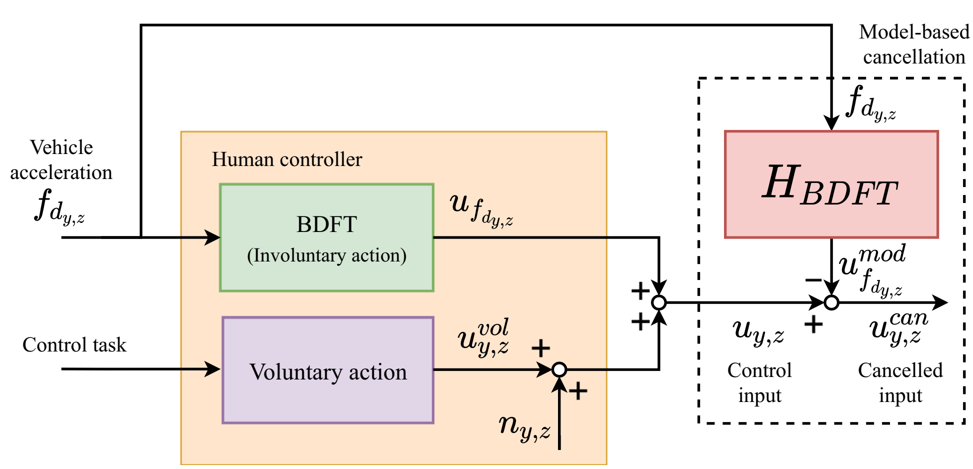


**Figure 1.** Definition of open-loop BDFT and model-based BDFT cancellation.

this is indicated with the green block that is driven by the vehicle acceleration disturbance signal $f_{d_{y,z}}$ and results in the BDFT input component $u_{f_{d_{y,z}}}$ (Venrooij, 2014). Note that for open-loop BDFT, as considered in this paper, the motion disturbance $f_{d_{y,z}}$ is independent from the control input $u_{y,z}$. Finally, completing a quasi-linear view on human pilot control behavior (McRuer & Jex, 1967; Mulder et al., 2018), Figure 1 indicates a remnant signal $n_{y,z}$, which accounts for the stochastic human-induced noise in $u_{y,z}$ that is not correlated with either the tracking signal or motion disturbance.

Figure 1 also shows the process of model-based BDFT cancellation, as investigated in this paper. The goal of model-based BDFT cancellation is to remove the contribution of the motion disturbances $f_{d_{y,z}}$ from the total control input $u_{y,z}$. In model-based BDFT cancellation, this is done by using a mathematical model of the human pilot's BDFT dynamics, indicated with the red $H_{BDFT}$ block in Figure 1. Using a measurement of the vehicle accelerations $f_{d_{y,z}}$, this model enables the prediction of the BDFT contribution to $u_{y,z}$, here indicated as $u^{mod}_{f_{d_{y,z}}}$. With the predicted BDFT contribution, the real BDFT contribution $u_{f_{d_{y,z}}}$ can be mitigated in the "cancelled" screen input signal $u^{can}_{y,z}$, which can be calculated as:

$$u^{can}_{y,z} = u_{y,z} - u^{mod}_{f_{d_{y,z}}} = \underbrace{u^{vol}_{y,z} + n_{y,z}}_{\text{Voluntary action}} + \underbrace{u_{f_{d_{y,z}}} - u^{mod}_{f_{d_{y,z}}}}_{\text{BDFT cancellation}} \tag{1}$$

With an accurate model of pilots' BDFT dynamics $H_{BDFT}$, the "BDFT cancellation" term in Eq. (1) will approximate zero. The model-based cancellation as shown in Figure 1 can be implemented in the software that interprets touchscreen inputs and gestures. This paper will focus on the key element in achieving successful model-based BDFT cancellation, i.e., the BDFT dynamics model $H_{BDFT}$ and the extent to which this model would need to be task- (and scenario-)dependent due to human pilots' adaptive neuromuscular systems (Mulder et al., 2018; Venrooij et al., 2010).

## 3. Method

### 3.1. Hypotheses

The following two hypotheses were formulated for the experiment:

**H1**: *For the multisine task, up to 88% of the BDFT can be canceled with the proposed model-based cancellation.* The BDFT dynamics are estimated from data for the performed multisine task, see Section 3.2.1. The success of model-based mitigation is directly linked to the quality of BDFT modeling. With the estimated BDFT models (see Section 3.3) showing even higher Variance Accounted For (VAF) values (88%) than those reported by Mobertz et al. (2018) (75%), for the multisine task a successful cancellation of 88% in terms of signal variance is expected. This is equivalent to a 65% attenuation (i.e., as 1-$\sqrt{1-0.88}$=0.65) of the true magnitude of $u_{f_{d_{y,z}}}$.

**H2**: *For the step task, BDFT cancellation based on multisine task BDFT models will be ineffective.* In earlier work in the context of sidestick manipulators (Venrooij et al., 2011), model-based BDFT mitigation has shown to be strongly dependent on the task, due to highly variable neuromuscular system settings adopted by pilots. Although no studies detail this relationship between neuromuscular settings and touchscreen tasks, the differences between the multisine (continuous dragging, Section 3.2.1) and step task (discrete dragging, Section 3.2.2) are expected to directly affect the cancellation. Moreover, as the screen input velocity goes toward zero, as in the step task, there is a possibility of nonlinear stick-slip, which can further degrade the applicability of the BDFT models (Robinson et al., 2014).

### 3.2. Control tasks

The direct manipulation capabilities of touchscreens are expected to facilitate point-to-point precision dragging as an essential input task on the future flight deck, for example, for flight plan modifications and waypoint relocations (Dodd et al., 2014; Mertens et al., 2012; Stuyven et al., 2012), but also for intuitive speed, altitude, and heading selection (Rouwhorst et al., 2017). For our human-in-the-loop experiment, we focused on two different touchscreen precision dragging tasks: a continuous multisine task and a discrete point-to-point step task (i.e., target acquisition). Both tasks only focused on dragging gestures and how BDFT affects dragging precision. Hence, participants' fingers were required to be in constant contact with the screen during the tasks. For dragging, the added arm stability from touching the screen already helps counter the effects of BDFT. Furthermore, this means that any BDFT effects occurring during the reaching for or pointing at a touchscreen, or when releasing a finger from the screen once a target is reached, were not accounted for in the experiment.

In both the multisine and step tasks, participants had to track the movement of a white target marker across the touchscreen, where the two-dimensional target movement was defined with horizontal and vertical target signals, $f_{t_y}$ and $f_{t_z}$, respectively. For both tasks the experiment runs lasted 90 seconds, of which the last 81.92 seconds were the measurement interval. While the multisine task was used for the identification of BDFT models ($H_{BDFT}$ in Figure 1), both tasks were also used for testing the effectiveness of the model-based BDFT cancellation while under the influence of motion disturbance signals. The tasks were performed on a touchscreen mounted in an upright position directly in front of the participant, typical of a primary flight display (PFD).

#### 3.2.1. Continuous multisine task

For the multisine task, the horizontal ($f_{t_y}$) and vertical ($f_{t_z}$) target screen positions were defined as sum-of-sine signals, resulting in a uninterrupted required movement across the screen. These signals were identical to those used by Mobertz et al. (2018) and consisted of three sines with distinct frequencies. The two-dimensional touchscreen target signals were meant to create a continuous and unpredictable task for the operator, without being too challenging. For a task that required participants to use the full extent of the touchscreen, see Figure 2, the vertical target had a root mean square displacement of 360 px (106.92 mm), while this was 480 px (142.56 mm) for the horizontal target. Figure 3 shows a sample time trace for the horizontal target signal $f_{t_y}$, as well as the corresponding recorded touchscreen input $u_y$. For reference, Table 1 lists all details of the $f_{t_y}$ and $f_{t_z}$ signals as also reported in (Mobertz et al., 2018).

#### 3.2.2. Discrete step task

The discrete step task was not used for BDFT model identification (see Sec. 3.3), but to explicitly assess the generalizability of the model-based BDFT approach for different touchscreen input tasks. The step task required repeated realistic precision dragging movements between two touchscreen locations. The target endpoint locations for the step task were concentric with respect to the center of the touchscreen. Figure 4 shows the four possible endpoint locations, which were chosen to be 500 px (148.5 mm) apart. The horizontal and vertical target signals $f_{t_y}$ and $f_{t_z}$ were designed such that the target marker would stay at a specific location for 3 seconds before shifting to one of the three other endpoints shown in Figure 4 . With the four possible endpoint locations in Figure 4, screen movements were thus limited to only vertical, horizontal and diagonal movements. Figure 5 shows a sample time trace of $f_{t_y}$ and a corresponding horizontal screen input $u_y$. The vertical target signal had a similar, interleaved, pattern of 3-second pulses. The 3-second stabilization at the target location was chosen empirically, as it was found that subjects needed between 1.0 and 1.5 seconds to move to the endpoint location.

#### 3.2.3. Motion disturbance signal

In our experiment, the motion disturbance signal $f_{d_{y,z}}$ (see Figure 1) was used to simulate motion accelerations representative for realistic turbulence, while at the same time enabling the retrieval of an estimate of participants' BDFT dynamics ($H_{BDFT}$) using frequency-domain system identification techniques (Damveld et al., 2013, 2010; Mobertz et al., 2018; Van Paassen & Mulder, 2006), see Sec. 3.3. To facilitate a fair comparison, the same disturbance signal was applied separately in the lateral ("sway") and vertical ("heave") motion axes, i.e., $f_{d_y} = f_{d_z} = f_d$. These conditions were chosen for two reasons. First, aircraft turbulence is mostly present in sway and heave (Hourlier et al., 2019). Furthermore, Mobertz et al. (2018) showed that strong biodynamic feedthrough is present for a touchscreen primary flight display in these conditions and that this enables reliable system identification of the BDFT dynamics. Based on earlier research (Mobertz et al., 2018; Zaal et al., 2009), the motion disturbance signal was defined as a multisine signal with sines at $N_d$ = 10 different frequencies ($\omega_d$), ranging between 0.38 and 17.33 rad/s:

$$f_d(t) = \sum_{k=1}^{N_d} A_d[k] \sin(\omega_d[k]t + \phi_d[k]) \tag{2}$$

To ensure a realistic feel, the signal's amplitude distribution $A_d$ was defined by a low-pass filter (Zaal et al., 2009), which gave reduced power at higher frequencies. To limit peaks in the time domain, the phases were chosen using a cresting technique (Damveld et al., 2010). Table 1 lists the numerical details of the disturbance signal, which was identical to that used by Mobertz et al. (2018). Please note that for convenience Table 1 reports the simulator displacement signal, $f_d^{pos}$, while for the BDFT modeling in this chapter we use the corresponding acceleration signal $f_d$.

### 3.3. BDFT modeling

In this paper, we focus on estimating models for BDFT for two different conditions where the directions of motion disturbance and screen input align: BDFT in horizontal touchscreen inputs due to sway (lateral) motion disturbances (denoted as HOR) and BDFT in vertical inputs due to heave (vertical) motion disturbances (denoted as VER). While motion disturbances will also affect input performance in other input directions (Mobertz et al., 2018), these BDFT contributions are less pronounced and also result in less accurate BDFT modeling results.

From the measured $f_{d_{y,z}}$ and $u_{y,z}$ experiment data, see Figure 1, a BDFT frequency response estimate $\hat{H}_{BDFT}(j\omega_d)$ was first estimated using a black-box frequency-domain identification approach as typically used for analysis of human control dynamics (McRuer & Jex, 1967; Mulder et al., 2018; Van Paassen & Mulder, 2006).

**Table 1.** Multisine properties used for the disturbance and multisine target signals.

| | Disturbance, $f_{d_{y,z}}^{pos}$ | | | | Horizontal target, $f_{t_y}$ | | | | Vertical target, $f_{t_z}$ | | | |
|---|---|---|---|---|---|---|---|---|---|---|---|---|
| $k$ | $n_d$ | $\omega_d$ | $A_d$ | $\phi_d$ | $n_{t_y}$ | $\omega_{t_y}$ | $A_{t_y}$ | $\phi_{t_y}$ | $n_{t_z}$ | $\omega_{t_z}$ | $A_{t_z}$ | $\phi_{t_z}$ |
| - | – | rad/s | mm | rad | – | rad/s | mm | rad | – | rad/s | mm | rad |
| 1 | 5 | 0.384 | 106.70 | −0.269 | 3 | 0.230 | 32.77 | 1.445 | 2 | 0.153 | 22.77 | 0.308 |
| 2 | 11 | 0.844 | 80.69 | 4.016 | 7 | 0.537 | 39.78 | 0.000 | 13 | 0.997 | 39.78 | −0.431 |
| 3 | 23 | 1.764 | 40.19 | −0.806 | 19 | 1.457 | 71.35 | −1.825 | 17 | 1.304 | 47.51 | −1.591 |
| 4 | 37 | 2.838 | 20.48 | 4.938 | | | | | | | | |
| 5 | 51 | 3.912 | 12.46 | 5.442 | | | | | | | | |
| 6 | 71 | 5.446 | 7.57 | 2.274 | | | | | | | | |
| 7 | 101 | 7.747 | 4.74 | 1.636 | | | | | | | | |
| 8 | 137 | 10.508 | 3.42 | 2.973 | | | | | | | | |
| 9 | 171 | 13.116 | 2.86 | 3.429 | | | | | | | | |
| 10 | 226 | 17.334 | 2.42 | 3.486 | | | | | | | | |

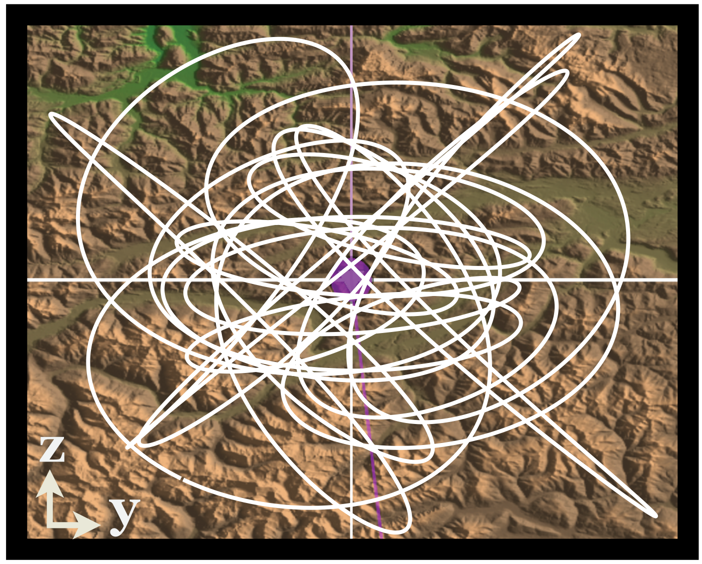


**Figure 2.** Display with the target location path for a single run across the touchscreen for the multisine task.

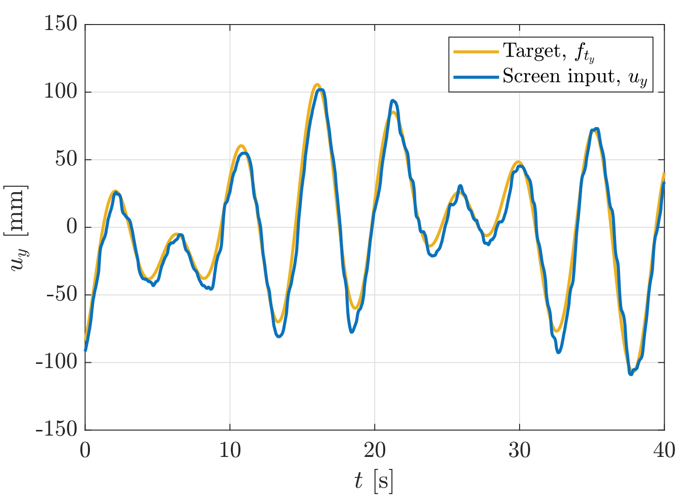


**Figure 3.** Example target $f_{t_y}$ and touchscreen input $u_y$ time traces for the multisine task.

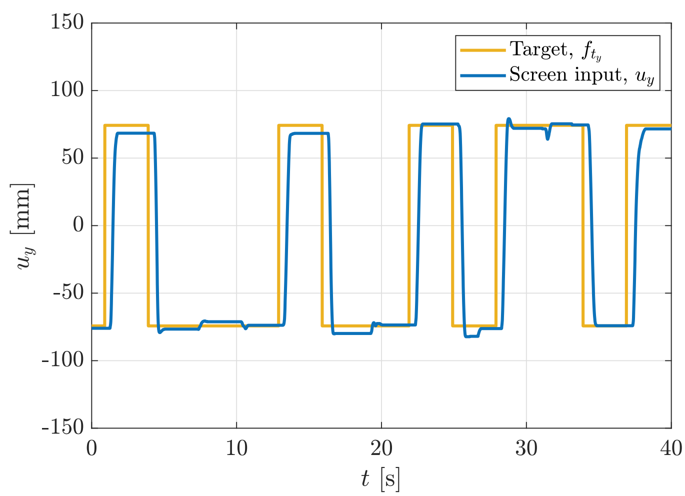


**Figure 5.** Example target $f_{t_y}$ and touchscreen input $u_y$ time traces for the step task.

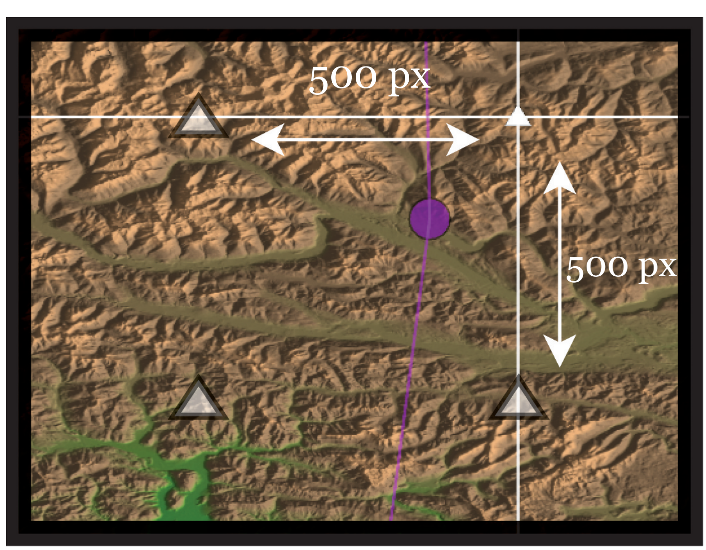


**Figure 4.** Display with possible target endpoint locations for the step task.

Based on earlier work (Mobertz et al., 2018; Venrooij et al., 2010), a second-order mass-spring-damper system with an additional gain $G_{BDFT}$ and a time delay $\tau_{BDFT}$ was then used for modeling participants' BDFT dynamics, see Eq. (3):

$$H_{BDFT}(s) = G_{BDFT} \frac{\omega_{BDFT}^2}{s^2 + 2\zeta_{BDFT}\omega_{BDFT}s + \omega_{BDFT}^2} e^{-s\tau_{BDFT}} \quad (3)$$

In the four-parameter model of Eq. (3), the gain $G_{BDFT}$ captures the magnitude of the BDFT response, which can be different between experiment conditions and individual participants. The second-order BDFT dynamics are parameterized with the natural frequency $\omega_{BDFT}$ and damping ratio $\zeta_{BDFT}$. Finally, the time delay $\tau_{BDFT}$ was added compared to (Mobertz et al., 2018) to further improve the high-frequency phase fit of the BDFT model compared to the identified $\hat{H}_{BDFT}(j\omega_d)$. The model of Eq. (3) describes all effects between the motion acceleration $f_{d_{y,z}}$ and the finger position $u_{y,z}$. Hence, the model lumps together several contributing systems such as the seat, spine, and arm dynamics acting in parallel to cause BDFT.

The Variance Accounted For (VAF) was used for model validation. The VAF indicates how much of the measured variance of a BDFT signal can be explained by the BDFT model of Eq. (3), where a VAF of 100% indicates that two signals are identical. Overall, the high VAF values obtained for both the HOR ($\mu$ = 87.9%, $\sigma$ = 3.9%) and VER conditions ($\mu$ = 74.0%, $\sigma$ = 16.5%) show that the model of Eq. (3) can model measured BDFT at high accuracy.

### 3.4. Apparatus

The experiment was performed in the SIMONA Research Simulator (SRS) at Delft University of Technology, see Figure 6. The SRS's 6-degree-of-freedom hexapod motion system was used to apply the motion disturbances, $f_{d_{y,z}}$. The experimental setup inside the SRS cockpit is shown in Figure 7. A 15-inch Iiyama ProLite TF1534MC-B1X capacitive touchscreen was installed directly in front of the pilot seat and was tilted 18 deg with respect to the vertical plane. It had a 1024 × 768 px resolution, a pixel pitch of 0.297 mm/px and a tap response time of 8 ms. The drag latency of the screen was measured with a custom test bench (Vrouwenvelder et al., 2021) and was found to be a function of input speed, which for the dragging tasks considered in our experiments meant a drag delay between 70 and 80 ms was present. The adjustable seat was equipped with a five-point harness, restricting the movement of the participants, but still allowing the upper body to lean forward. The light in the cabin was kept on throughout the experiment to reduce eye strain. To reduce friction and finger fatigue, the participants wore anti-static gloves for the duration of the experiment (EN338 performance level 2242, NEN-EN-IEC 61340-5-1 ESD rated).

### 3.5. Participantsand procedures

The experiment was performed by 18 participants ($\mu$ = 27 years, $\sigma$ = 4.77 years) of which 15 were male and 3 female. All were recruited from the student population at Delft University of Technology. None of the participants were pilots or had extensive prior experience with turbulent aircraft motion from, e.g., earlier simulator experiments. For reference, the participants' height ($\mu$ = 179.7 cm, $\sigma$ = 7.3 cm) and weight ($\mu$ = 78.5 kg, $\sigma$ = 12.7 kg) were measured and used to derive the Body-Mass-Index (BMI) ($\mu$ = 24.3 kg/m$^2$, $\sigma$ = 3.6 kg/m$^2$). Participants were asked to use their dominant hand during the experiment (1 left-handed, 17 right-handed). All participants provided written informed consent prior to taking part in the experiment.


Figure 6. The SIMONA Research Simulator (SRS).

### 3.6. Experiment procedures

A written briefing was sent to the participants a couple of days before the experiment, explaining the tasks and experiment procedures. The experiment was split over two sessions performed on different days, see Figure 8 . In the first session on Day 1 participants performed the multisine task with both lateral (Y) and vertical (Z) motion disturbances (8 runs each). Both conditions were presented in a randomized order and a short break of around 10 minutes was taken after the first 8 runs. The data from the second half of Day 1 was used for estimating the BDFT models (see Sec. 3.3).

The second session on Day 2, see Figure 8, was used to evaluate the effectiveness of model-based BDFT mitigation in both the multisine and step tasks. The number of days between sessions varied between 3 and 14 days for different

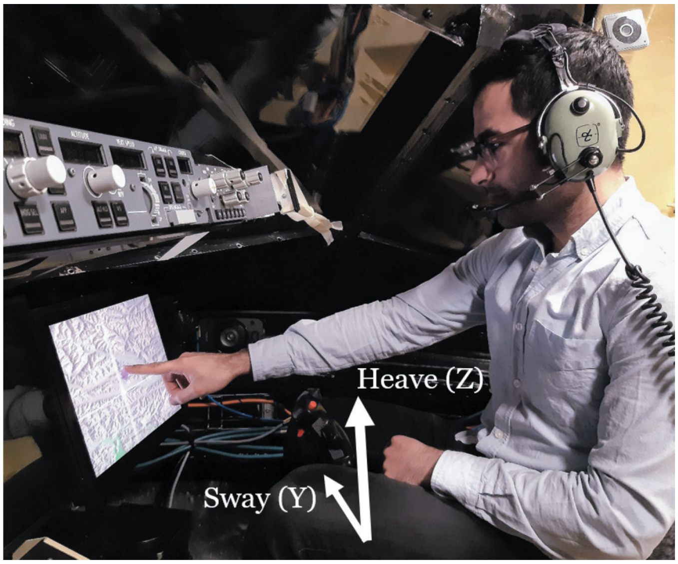


Figure 7. SRS flight deck experiment setup.

participants. At the start of Day 2, participants received two training runs with no motion disturbance (NM) to (re)familiarize themselves with the multisine task and the new step task. In the "Cancellation" part of the second session, participants performed both tasks with the same lateral and vertical motion disturbances also used for the first session. In addition, they performed both tasks in a no-motion condition NM, to collect reference BDFT-free task performance data. All six conditions were repeated four times (24 runs total), presented in randomized order using a randomized Latin square, with a small break after the first 12 runs. Throughout the second session, the participants were never aware of the BDFT cancellation occurring, as the mitigation is implemented in the post-hoc touch input processing step (see Figure 1) and no additional (visual) feedback of its effect was provided to the participants.

In both experiment sessions, the experimenter monitored participants' task performance (root mean square difference between target and finger screen positions). No explicit task performance feedback was provided to the participants. However, the experimenter gave verbal motivational encouragement in cases where participants lost focus or experienced arm fatigue.

## 4. Results

### 4.1. BDFT modeling

Figure 9 shows the estimated parameters of the BDFT model in Eq. (3) for both the HOR and VER conditions. Each boxplot shows the variation in BDFT model parameters across all participants, with the average values as used for performing model-based BDFT cancellation in the second experiment session indicated with red asterisks.

Figure 9 shows that the estimates of the BDFT model parameters are consistent across participants and that differences in BDFT dynamics occur between the HOR and VER conditions, as expected. Figure 9(a) shows a reduced BDFT gain, $G_{BDFT}$, for the VER condition, which is in line with previous research where stronger feedthrough of sway motion to horizontal screen inputs (HOR) compared to the effects of heave accelerations on vertical screen inputs (VER) was also found (Mobertz et al., 2018). The BDFT dynamics' natural frequency $\omega_{BDFT}$ (see Figure 9(b)) is found to be equivalent, with an average value of 7 rad/s, for both conditions. For the damping ratio $\zeta_{BDFT}$, see Figure 9(c), average values of 0.69 and 0.95 were found for HOR and VER, respectively. Finally, the time delay $\tau_{BDFT}$ was found to be 25 ms higher for the HOR condition than for VER. Because the BDFT model of Eq. (3) is a lumped model, a direct explanation for the parameter differences between the HOR and VER conditions is not straightforward. However, vibrations in sway have been shown to have fundamentally different biodynamic effects compared to vertical vibrations because of the movement of the hip joint and bending of the spine (Allen et al., 1973). This difference is indeed consistent with the increased latency ($\tau_{BDFT}$) and the lower damping ratio ($\zeta_{BDFT}$) found for the HOR condition.

### 4.2. BDFT cancellation

#### 4.2.1. Continuous multisine task

Figure 10 shows example time traces illustrating the effectiveness of the model-based BDFT cancellation for both the HOR and VER conditions. In these figures, the horizontal/vertical target signals are shown in yellow, while the corresponding (raw) touchscreen input is shown in blue. Also, the result of the model-based cancellation, i.e., $u^{can}_{y,z}$ as defined by Eq. (1), is

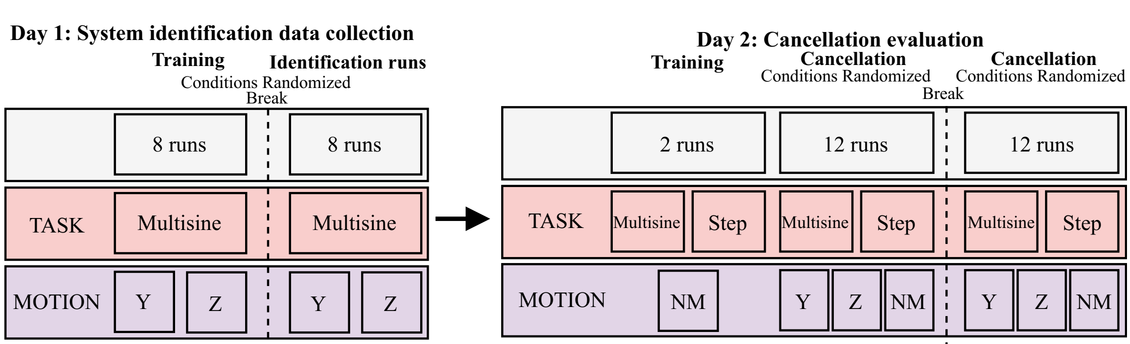


Figure 8. Overview of tested experiment conditions and procedures.

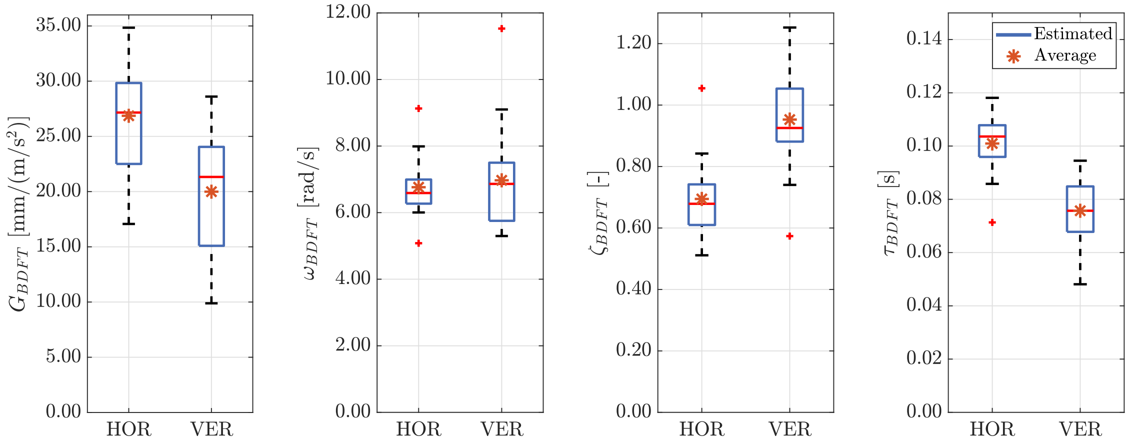


(a) Gain (b) Natural frequency (c) Damping ratio (d) Time delay

**Figure 9.** Estimated BDFT model parameters.

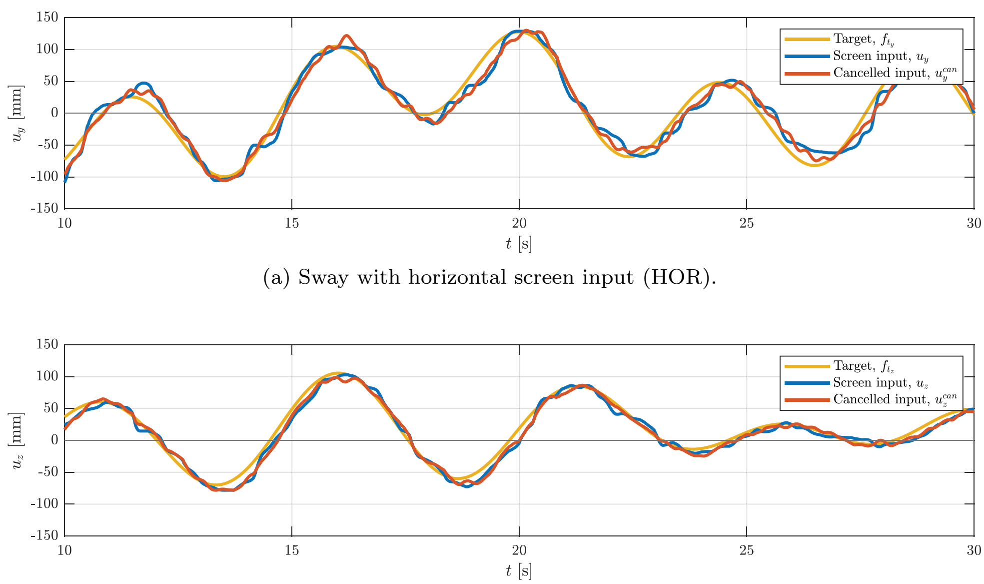


(a) Sway with horizontal screen input (HOR).

(b) Heave with vertical screen input (VER).

**Figure 10.** Typical time traces for the multisine task with BDFT cancellation in both the HOR and VER conditions (Participant 1, Trial 1).

shown in red. While Figure 10 only shows an example result for trial 1 of the multisine task performed by Participant 1, equivalent results were obtained for all other participants and repeated trials.

Figure 10 shows that the canceled input signal $u_{y,z}^{can}$ shows reduced high-frequency oscillations compared the corresponding $u_{y,z}$, on average. This suggests successful model-based BDFT cancellation, as it seems the $f_{d_{y,z}}$ component in $u_{y,z}$ was mitigated effectively. To further quantify this improvement, Figure 11 shows the standard deviation (i.e., average magnitude over time) of the disturbance component in $u_{y,z}$, i.e., $\sigma\{u_{f_{d_{y,z}}}\}$. The boxplots show this data across all experiment participants for the reference no-motion condition as well as the original and canceled results for the respective motion conditions. Note that for clarity, the color of the boxplots in Figure 11 matches the line color in Figure 10 .

The no-motion condition data in Figure 11 shows that without motion disturbances the magnitude of $\sigma\{u_{f_{d_{y,z}}}\}$ is negligible, as no BDFT occurs in this condition. For both HOR and VER with cancellation off (blue data in Figure 11), the BDFT component in $u_{y,z}$ is seen to be considerable, with standard deviations of 8.5 mm and 5.1 mm, respectively. As also reported for the BDFT gain results in Figure 9, the fact that more BDFT occurs for the HOR condition is indicative of increased susceptibility to BDFT for lateral disturbances and consistent with earlier research (Mobertz et al., 2018). With the model-based cancellation active (red data in Figure 11), the BDFT component is seen to be suppressed to 3.0 mm and 1.9 mm average standard deviations for HOR and VER, respectively. While clearly still motion disturbance power is present in comparison with the no-motion data, an effective reduction in $\sigma\{u_{f_{d_{y,z}}}\}$ of around 63% is achieved for both conditions. As explained for Hypothesis H1 in Sec. 3.1, this closely matches the expected result (65%) for cancellation with a BDFT model that explains the BDFT component in $u_{y,z}$ with a VAF of around 88%.

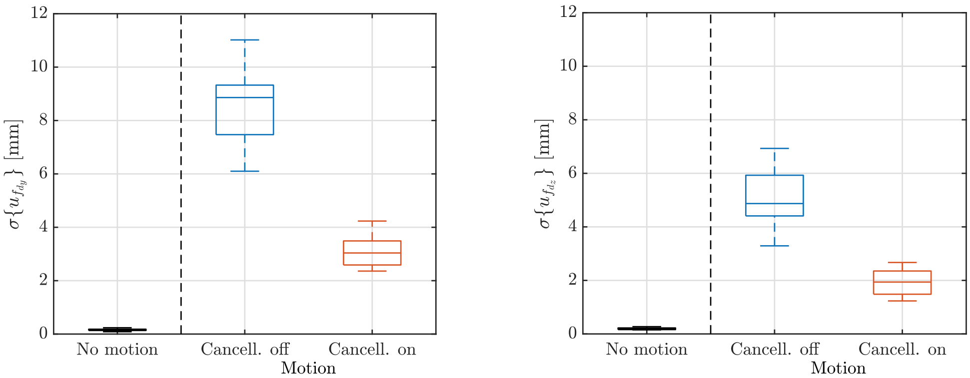


(a) Sway with horizontal screen input (HOR). (b) Heave with vertical screen input (VER).

**Figure 11.** Comparison of the standard deviation of the disturbance component in the input signal $\sigma\{u_{f_{d_{y,z}}}\}$ for the multisine task.

### 4.2.2. *Discrete step task*

In Sec. 4.2.1, BDFT models that were identified from a multisine pursuit task data, were applied for BDFT cancellation in that same task, resulting in an effective BDFT reduction. To verify the generalizability of the BDFT model that is essential for model-based BDFT cancellation, here the same BDFT models are applied for cancellation in the step task detailed in Sec. 3.2.2 . Matching the results presented for the multisine task in Figures 10 and 11, Figures 12 and 13 show example single-trial time traces for a single participant (Participant 1, Trial 1) and average cancellation performance indicators, respectively. Please note that in Figure 13 we consider a different performance indicator than shown in Figure 11: for the step task we compare the overall standard deviation of the touch input data at the endpoint locations of each step, i.e., $\sigma\{u_{y,z}\}$, as with steps the contribution of $f_{d_{y,z}}$ cannot be reliably separated in the frequency domain (Mulder et al., 2018; Pool et al., 2011). The shaded areas in Figure 12 indicate the time segments where the BDFT cancellation performance was assessed, i.e., the last 1.5 seconds of each 3-second dwell time on a new target location.

Figure 12 shows example time-domain data for the step task for both the VER and HOR conditions. As is clear from these figures, the raw touch input (blue data) shows that participants were able to accurately hold their fingers at the endpoint location despite being perturbed by $f_{d_{y,z}}$. Using the BDFT model and the measured motion disturbance signal to calculate the canceled input signal ($u^{can}_{y,z}$) according to Eq. (1) is seen to result in significantly more oscillations around the target endpoints and thus an amplification of BDFT-related errors compared to the raw input. This result was consistent across all participants in the experiment, as shown in Figure 13, where, matching Figure 11, the presence of a motion disturbance without cancellation (blue data) is seen to result in an increase in endpoint variation compared to the no-motion case. However, unlike the result obtained for the multisine task, with the model-based cancellation active the standard deviation

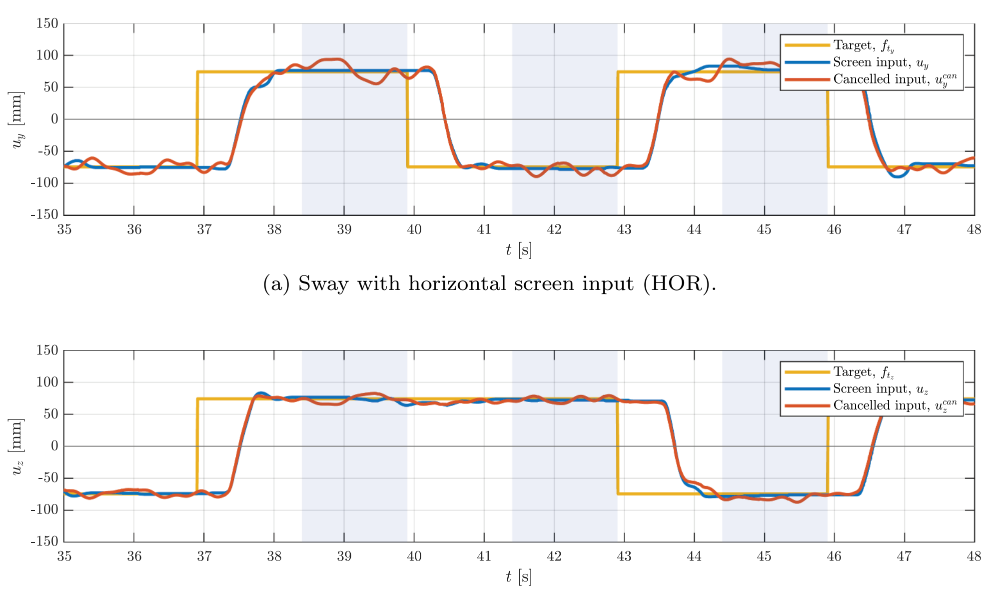


(a) Sway with horizontal screen input (HOR).

(b) Heave with vertical screen input (VER).

**Figure 12.** Typical time traces for the step task with BDFT cancellation in both the HOR and VER conditions (Participant 1, Trial 1). The shaded areas indicate the stabilized endpoint data that were used for cancellation assessment.

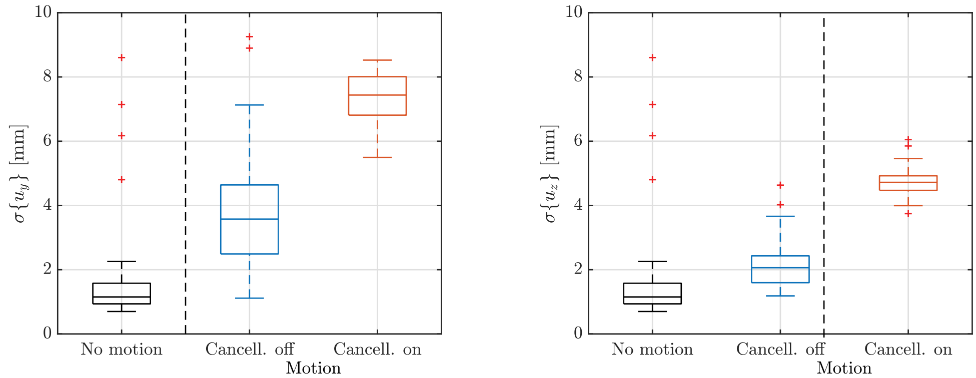


(a) Sway with horizontal screen input (HOR). (b) Heave with vertical screen input (VER).

**Figure 13.** Comparison of step task endpoint variation with and without model-based cancellation.

of the endpoint touch inputs $\sigma\{u_{y,z}\}$ is seen to be increased further with a factor 2 or more, on average. This confirms the expectation formulated in Hypothesis H2 that due to neuromuscular adaptation to the performed touchscreen task also the BDFT dynamics that would need to be canceled are strongly task-dependent.

The results in Figures 12 and 13 were not unexpected, as the susceptibility to BDFT is less when keeping a finger at a fixed screen location than when performing a dynamic dragging motion. To include such task-adaptive effects in the model-based cancellation, the parameters of the BDFT model (i.e., $G_{BDFT}$, $\omega_{BDFT}$, $\zeta_{BDFT}$, and $\tau_{BDFT}$) could be updated. Figure 14 shows again the average standard deviation in touch endpoint position ($\sigma\{u_{y,z}\}$) where the BDFT model gain is varied over a representative range. The $G_{BDFT}$ values estimated from the multisine data for both the HOR and VER conditions are indicated in Figure 14 with a vertical dashed red line. The horizontal black lines show the average $\sigma\{u_{y,z}\}$ values for the no-motion and no-cancellation data from Figure 13. The red line shows the resulting endpoint variation with cancellation on as a function of $G_{BDFT}$, where the shaded area indicates the standard deviation across the four repeated experiment runs. Figure 14 shows that for both the HOR and VER conditions the model-based cancellation can be made effective with a reduced BDFT model gain. For HOR an optimum is reached at $G_{BDFT}$ = 5 mm/(m/s$^2$), while for VER the optimum is at $G_{BDFT}$ = 3 mm/(m/s$^2$). Both on average result in a 12% decrease in $\sigma\{u_{y,z}\}$ compared to having the cancellation off. Thereby Figure 14 shows that even by adapting only one of the BDFT model parameters the model-cancellation can still be effective for a different task.

## 5. Discussion

With touchscreen devices being foreseen as an integral part of the future commercial flight deck, this paper focused on a key problem in operating touchscreens in a moving and vibratory environment such as an aircraft: biodynamic feedthrough (BDFT). This paper described a human-in-the-loop experiment performed to test the feasibility of model-based BDFT cancellation for touchscreens under turbulent conditions. In a first experiment session, 18 participants performed a two-dimensional continuous dragging task under the influence of a multisine motion disturbance signal resembling turbulence, allowing for the identification of (transfer function) BDFT models. In a second experiment session, the estimated models were used to perform BDFT cancellation in the same continuous multisine task, as well as a discrete step task. Thus, this experiment allowed for investigating the potential of model-based BDFT cancellation and the effectiveness of the cancellation across different touchscreen tasks.

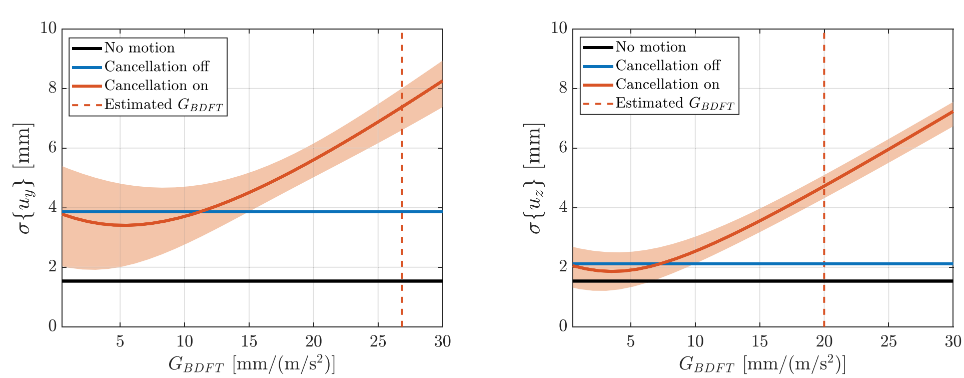


(a) Sway with horizontal screen input (HOR). (b) Heave with vertical screen input (VER).

**Figure 14.** Step task endpoint variation for varying $G_{BDFT}$.

In a precursor study, Mobertz et al. (2018) showed that BDFT touchscreen inputs during a continuous input task could be modeled at high accuracy using a linear transfer function model. To achieve a further improved model fit to the current experiment data, a time delay was added to the BDFT model, resulting in BDFT model VAF values up to 88% on average. Based on these results, Hypothesis **H1** predicted that for the continuous multisine task, also used for BDFT model identification, up to 65% of the BDFT component in the registered touch inputs could be removed. The experiment data showed that indeed a cancellation of around 63% was achieved on average for both the HOR and VER conditions. As this shows that a major portion of BDFT can indeed be canceled for both lateral and vertical motion disturbances, Hypothesis H1 is accepted. Furthermore, as this result was obtained with "one-size-fits-all" BDFT models for which the average BDFT parameters across all experiment participants were used, this result can likely straightforwardly be improved by using more *personalized* BDFT models that better capture the biodynamic properties of individual pilots. Investigations into model-based BDFT mitigation with physical control inceptors (Venrooij et al., 2011) have shown that such personalized BDFT models can indeed enable a substantially enhanced effectiveness of this approach.

The main goal of the performed experiment was to not only verify the effectiveness of model-based BDFT mitigation in the same (continuous multisine) task, but also its applicability to a different, more realistic, precision dragging (discrete step) task. As stated in Hypothesis **H2**, based on expected differences in neuromuscular and biodynamic settings across tasks, it was expected that worse cancellation would occur when applying the BDFT model estimated from the continuous multisine task to a touchscreen step task. Although different metrics to quantify BDFT cancellation performance were used between tasks, the cancellation in the step task was clearly found to be ineffective and in fact amplified the effects of BDFT while participants' fingers were at the target screen location. Thus, Hypothesis H2 is also accepted. This is explained by the fact that neuromuscular dynamics, and hence also BDFT dynamics, vary with task demands. For true point-to-point dragging such as performed in our step task, BDFT during the (short) dragging movement is equivalent to the BDFT measured in our multisine task. However, once at the endpoint location more pressure can be applied on the screen to stabilize the hand motion and reduce BDFT. In addition, most participants indeed rolled or pivoted around their finger to keep the contact point in the same location. In other words, once a stationary endpoint is reached, the task becomes a pure disturbance-rejection task, with a singular focus on reducing the biodynamic feedthrough. In a directed dragging motion, however, participants perform a combined target-following and disturbance-rejection task, involving a trade-off between accurately following the target and minimizing the effects of BDFT. These results imply that model-based BDFT cancellation will need to be made adaptive to the task in order to be effective.

The experiments described in this paper explicitly measured how turbulence affects dragging movements on a touchscreen, which is widely believed to be an essential input task on the future flight deck (Dodd et al., 2014; Mertens et al., 2012; Stuyven et al., 2012). The two tasks tested in the experiment were designed to enable the accurate measurement of realistic BDFT effects on touchscreen dragging, not to directly mimic a realistic flight deck task. For example, in our multisine task participants performed a continuous dragging task, i.e., a single uninterrupted 90-second dragging movement across the touchscreen. The step task was a more faithful representation of a realistic precision input task, such as a flight plan modification (Alapetite et al., 2012; Mertens et al., 2012; Rouwhorst et al., 2017; Stuyven et al., 2012), but still included an (unrealistically) large number of dragging movements to improve the data density. Similarly, while it was designed to match the frequency spectrum of realistic turbulence-induced aircraft motion (Mobertz et al., 2018), the (multisine) motion disturbance signal that simulated turbulence accelerations in our experiments was not, in itself, a realistic simulation of turbulence. These choices, all made to facilitate our detailed analysis of BDFT dynamics, perhaps resulted in limited ecological validity of the tested tasks themselves. However, as the low-level perturbation of human arms due to cockpit accelerations will not fundamentally change, the measured BDFT dynamics and cancellation results as presented here can still be considered representative. The true generalizability of our results can, for example, be assessed by evaluating our model-based mitigation methodology, with real pilots, in a combined simulator and in-flight experiment.

Toward further development of practical model-based BDFT cancellation for touchscreens, developing approaches to adapt the BDFT model that is used to predict the touch inputs due to BDFT, in *real time*, is a critical next step. As shown in this paper, using task-dependent parameters – i.e., a reduction in the gain of the BDFT model ($G_{BDFT}$) in the step task, resulting in an average BDFT reduction of 12% instead of a factor 2 amplification – can be sufficient to render a mismatched mitigation effective again. Potential approaches that can facilitate real-time adaptation of BDFT model parameters are, for example, explicit online estimators for the BDFT model's parameters (Olivari et al., 2014; Plaetinck et al., 2019) or predictive methods based on motion tracking (Ahmad et al., 2018).

Model-based cancellation of BDFT has the benefit of being a purely software-based approach that only requires measured data (i.e., lateral and vertical accelerations in the cockpit) that are generally available from inertial sensors in most aircraft. Unlike BDFT-mitigation techniques that require additional certified cockpit hardware (e.g., traditional hand-stabilizers), model-based BDFT mitigation can be implemented, cost-effectively, through updates to touchscreens' driver or gesture-interpretation software. This implies model-based BDFT mitigation is not only a technique that can help improve the future flight deck, but that also has potential for implementation, through retroactive updates, in existing aircraft.

While explicit requirements for a technique like model-based BDFT mitigation for cockpit touchscreens do not exist (FAA, 2011; SAE International, 2019), for touchscreens in the cockpit the FAA currently requires that under any circumstances "*The location of the pilot's finger touch, as sensed by the touch screen, should be predictable and obvious*"(FAA, 2011). As model-based BDFT mitigation techniques would involve modification of pilots true touch input in software processing, this is a key requirement to consider for this approach. In the experiment described in this paper, no (visual) feedback (e.g., corrected cursor position) was provided to participants. Hence, in our experiment the participants were not at all aware of the BDFT cancellation. As successful placement and dragging of an object is expected to be an essential operation on touchscreens on the future flight deck (Mertens et al., 2012; Stuyven et al., 2012) for which this would naturally become noticeable, ensuring that the FAA's advisory is met is a critical next step, and will be tested in future experimental work.

## 6. Conclusion

This paper presents the results of an experiment with 18 participants performed to investigate the mitigation of erroneous inputs due to biodynamic feedthrough (BDFT) in touchscreen dragging tasks. For this, we propose a novel model-based cancellation approach, that removes BDFT components from recorded touch inputs (in online software touch data processing) using a BDFT model that predicts erroneous finger movement based on measured cockpit accelerations. From our experiment data, accurate BDFT models that accounted for at least 74% of BDFT input data were identified for both horizontal BDFT inputs due to lateral vehicle accelerations (HOR) and vertical BDFT inputs due to vertical accelerations (VER). With averaged model parameters, the HOR and VER BDFT models were implemented for model-based BDFT cancellation in two different tasks: the continuous (multisine) dragging task also used for BDFT model identification, as well as a discrete point-to-point (step) dragging task. As expected, the approach was successful for mitigating BDFT in the continuous multisine task, resulting in a reduction of BDFT-related touch inputs of 63% on average. Using the same BDFT models for mitigation in the discrete step task was found to result in amplification of BDFT inputs rather than their attenuation. This was explained by the fact that in this task participants showed less BDFT, due the task allowing them to press their fingers more firmly on the screen and pivoting of the fingertip around the pressing point when at a stationary touch location. However, with only a task-adaptive adjustment of the BDFT models' gain parameters, still a 12% reduction in BDFT for both the HOR and VER conditions was obtained. Overall, the results show that model-based BDFT cancellation can be effective for touchscreen operation on the flight deck, but also confirm earlier findings in that BDFT is directly affected by how the finger is moved over the screen, resulting in limited task-to-task generalizability of the models used for this type of BDFT cancellation.

## ORCID

Daan M. Pool http://orcid.org/0000-0001-9535-2639

## References


Ahmad, B. I., Langdon, P. M., & Godsill, S. J. (2018). Stabilising touch interactions in cockpits, aerospace, and vibrating environments. In M. Antona & C. Stephanidis (Eds.), *Universal access in human-computer interaction. methods, technologies, and users* (pp. 133–145). Cham. Springer International Publishing.

Airbus (2019). *Airbus begins deliveries of first A350s with touchscreen cockpit displays option to customers.* Airbus S.A.S. https://www.airbus.com/newsroom/press-releases/en/2019/12/airbus-begins-deliveries-of-first-a350s-with-touchscreen-cockpit-displays-option-to-customers.html

Alapetite, A., Fogh, R., Zammit-Mangion, D., Zammit, C., Agius, I., Fabbri, M., Pregnolato, M., & Becouarn, L. (2012). Direct tactile manipulation of the flight plan in a modern aircraft cockpit. *Proceedings of HCI Aero*, 2–5.

Allen, R. W., Jex, H. R., & Magdaleno, R. E. (1973). *Manual control performance and dynamic response during sinusoidal vibration*. Technical report, System Technology Inc.

Avsar, H. (2017). *Exploring potential benefits and challenges of touch screens on the flight deck*. [PhD thesis, University of Nottingham].

Banerjee, D., Jordan, L. M., & Rosen, M. J. (1996). Modeling the effects of inertial reactions on occupants of moving power wheelchairs. *Proceedings of the Rehabilitation Engineering and Assistive Technology Society of North America Conference (RESNA)*, 220–222.

Bauersfeld, K. G. (1992). *Effects of turbulence and activation method on touchscreen perfor- mance in aviation environments*. [Master's thesis, San Jose State University].

Cockburn, A., Gutwin, C., Palanque, P., Deleris, Y., Trask, C., Coveney, A., Yung, M., & MacLean, K. (2017). Turbulent touch: Touchscreen input for cockpit flight displays. *Proceedings of the 2017 CHI Conference on Human Factors in Computing Systems*, CHI '17, (pp. 6742–6753). New York, NY, USA: ACM.

Cockburn, A., Masson, D., Gutwin, C., Palanque, P., Goguey, A., Yung, M., Gris, C., & Trask, C. (2019). Design and evaluation of braced touch for touchscreen input stabilisation. *International Journal of Human-Computer Studies*, *122*, 21–37. https://doi.org/10.1016/j.ijhcs.2018.08.005

Damveld, H. J., Abbink, D. A., Mulder, M., Mulder, M., Van Paassen, M. M., Van Der Helm, F. C. T., & Hosman, R. (2013). Identification of the Feedback Components of the Neuromuscular System in a Pitch Control Task. *AIAA Modeling and Simulation Technologies Conference*, Reston, Virigina: American Institute of Aeronautics and Astronautics.

Damveld, H. J., Beerens, G. C., Van Paassen, M. M., & Mulder, M. (2010). Design of forcing functions for the identification of human control behavior. *Journal of Guidance, Control, and Dynamics*, *33*(4), 1064–1081. https://doi.org/10.2514/1.47730

Dodd, S., Lancaster, J., Miranda, A., Grothe, S., DeMers, B., & Rogers, B. (2014). Touch screens on the Flight Deck: The impact of touch target size, spacing, touch technology and turbulence on pilot performance. *Proceedings of the Human Factors and Ergonomics Society Annual Meeting*, *58*(1), 6–10. https://doi.org/10.1177/1541931214581002

FAA (2011). *Advisory circular 20-175: Controls for flight deck systems*. Technical report, Federal Aviation Administration.

Gauci, J., Cauchi, N., Theuma, K., Zammit-Mangion, D., & Muscat, A. (2015). Design and evaluation of a touch screen concept for pilot interaction with avionic systems. *2015 IEEE/AIAA 34th Digital Avionics Systems Conference (DASC)*.

Gillespie, R. B., Hasser, C., & Tang, P. (1999). Cancellation of feedthrough dynamics using a force-reflecting joystick. *Proc. ASME Dynamic Systems and Controls Division*, 319–326.

Griffin, M. J. (2001). The validation of biodynamic models. *Clinical Biomechanics*, *16*, S81–S92. https://doi.org/10.1016/S0268-0033(00)00101-7

Hourlier, S., Guérard, S., & Servantie, X. (2019). Avionics touch screen in turbulence: Simulator design and selected human–machine interface metrics. In Michael A. Vidulich, & Pamela S.

Tsang (Eds.), *Improving aviation performance through applying engineering psychology: Advances in aviation psychology* (Vol. 3, pp. 53–75). CRC Press.

Humphreys, H. C., Book, W. J., & Huggins, J. D. (2010). Modeling of biodynamic feedthrough in backhoe operation. *Proceedings of the ASME Dynamic Systems and Control Conference 2009, DSCC2009*, 969–976.

Jex, H. R. (1972). Problems in modeling man-machine control behavior in biodynamic environments. In *Proceedings of the 7th Annual Conference on Manual Control*, 3–13.

Kaminani, S. (2011). Human computer interaction issues with touch screen interfaces in the flight deck. *Proceedings of the AIAA/IEEE Digital Avionics Systems Conference*, Seattle (WA).

Kingsley-Jones, M. (2018). *Airbus aims for airliner cockpit-touchscreen first with A350*. DVV Media International Ltd. https://www.flightglobal.com/news/articles/airbus-aims-for-airliner-cockpit-touchscreen-first-449481/

Lancaster, J., Mers, B., Rogers, B., Smart, A., & Whitlow, S. (2011). 57.3: The effect of touch screen hand stability method on performance & subjective preference in turbulence. *SID Symposium Digest of Technical Papers*, *42*(1), 841–844. https://doi.org/10.1889/1.3621464

Masarati, P., Quaranta, G., Bernardini, A., & Guglieri, G. (2015). Voluntary pilot action through biodynamics for helicopter flight dynamics simulation. *Journal of Guidance, Control, and Dynamics*, *38*(3), 431–441. https://doi.org/10.2514/1.G000837

Mayo, J. R. (1989). The involuntary participation of a human pilot in a helicopter. In *15th Eur. Rotorcraft Forum* (pp. 81–100). Amsterdam.

McRuer, D. T., & Jex, H. R. (1967). A review of quasi-linear pilot models. *IEEE Transactions on Human Factors in Electronics*, *HFE-8*(3), 231–249. https://doi.org/10.1109/THFE.1967.234304

Mertens, M. M., Damveld, H. J., & Borst, C. (2012). An avionics touch screen-based control display concept. In Peter L. Marasco, Paul R. Havig II, Daniel D. Desjardins, & Kalluri R. Sarma (Eds.), *Head- and helmet-mounted displays XVII; and display technologies and applications for defense, security, and avionics VI* (Vol. 8383). SPIE. https://doi.org/10.1117/12.919217

Mobertz, X., Pool, D. M., Van Paassen, M. M., & Mulder, M. (2018). A cybernetic analysis of biodynamic effects in touchscreen operation in turbulence. *2018 AIAA Modeling and Simulation Technologies Conference*, AIAA SciTech Forum. American Institute of Aeronautics and Astronautics.

Mulder, M., Pool, D. M., Abbink, D. A., Boer, E. R., Zaal, P. M. T., Drop, F. M., Van Der El, K., & Van Paassen, M. M. (2018). Manual control cybernetics: State-of-the-art and current trends. *IEEE Transactions on Human-Machine Systems*, *48*(5), 468–485. https://doi.org/10.1109/THMS.2017.2761342

Olivari, M., Nieuwenhuizen, F. M., Bülthoff, H. H., & Pollini, L. (2014). Identifying timevarying neuromuscular system with a recursive least-squares algorithm: A monte-carlo simulation study. In *Proceedings of the 2014 IEEE International Conference on Systems, Man, and Cybernetics*, (pp. 3573–3578). San Diego (CA).

Plaetinck, W., Pool, D. M., Van Paassen, M. M., & Mulder, M. (2019). Online identification of pilot adaptation to sudden degradations in vehicle stability. In *Proceedings of the 2nd IFAC Conference on Cyber-Physical & Human-Systems*, (pp. 347–352). Miami (FL), IFAC-PapersOnLine. 51.

Pool, D. M., Zaal, P. M. T., Van Paassen, M. M., & Mulder, M. (2011). Identification of multimodal pilot models using ramp target and multisine disturbance signals. *Journal of Guidance, Control, and Dynamics*, *34*(1), 86–97. https://doi.org/10.2514/1.50612

Robinson, T., Grabski, G., Green, J., Jacobson, M., Byrne, C., & Harper, D. (2014). P-171: Physical touch aspects of the touch interface for flight deck applications. *SID Symposium Digest of Technical Papers*, *45*(1), 1618–1621. https://doi.org/10.1002/j.2168-0159.2014.tb00432.x

Rouwhorst, W., Verhoeven, R., Suijkerbuijk, M., Bos, T., Maij, A., Vermaat, M., & Arents, R. (2017). Use of touch screen display applications for aircraft flight control. *2017 IEEE/AIAA 36th Digital Avionics Systems Conference (DASC)*, (pp. 1–10). IEEE.

SAE International. (2019). *Touch interactive display systems: Human factors considerations, system design and performance guidelines*. SAE International. https://doi.org/10.4271/ARP60494.

Sirouspour, M. R., & Salcudean, S. E. (2003). Suppressing operator-induced oscillations in manual control systems with movable bases. *IEEE Transactions on Control Systems Technology*, *11*(4), 448–459. https://doi.org/10.1109/TCST.2003.813386

Sövényi, S., & Gillespie, R. B. (2007). Cancellation of biodynamic feedthrough in vehicle control tasks. *IEEE Transactions on Control Systems Technology*, *15*(6), 1018–1029. https://doi.org/10.1109/TCST.2007.899679

Stuyven, G., Damveld, H. J., & Borst, C. (2012). Concept for an avionics multi touch Flight Deck. *SAE International Journal of Aerospace*, *5*(1), 164–171. https://doi.org/10.4271/2012-01-2120

Trimble, S. (2016). *Boeing selects Rockwell Collins for 777X touchscreens*. DVV Media International Ltd. https://www.flightglobal.com/news/articles/boeing-selects-rockwell-collins-for-777x-touchscreen-429565/

Van Paassen, M. M., & Mulder, M. (2006). Identification of human control behavior. In Waldemar Karwowski (Eds.), *International encyclopedia of ergonomics and human factors* (pp. 400–407). CRC Press.

Venrooij, J. (2014). *Measuring, modeling and mitigating biodynamic feedthrough*. [PhD thesis,Delft University of Technology].

Venrooij, J., Mulder, M., Abbink, D. A., Van Paassen, M. M., Van Der Helm, F. C. T., Bülthoff, H. H., & Mulder, M. (2013). A new view on biodynamic feedthrough analysis: Unifying the effects on forces and positions. *IEEE Transactions on Cybernetics*, *43*(1), 129–142. https://doi.org/10.1109/TSMCB.2012.2200972

Venrooij, J., Mulder, M., Van Paassen, M. M., Abbink, D. A., Bülthoff, H. H., & Mulder, M. (2011). Cancelling biodynamic feedthrough requires a subject and task dependent approach. *2011 IEEE International Conference on Systems, Man, and Cybernetics*, 1670–1675.

Venrooij, J., Mulder, M., Van Paassen, M. M., Mulder, M., & Abbink, D. A. (2010). A review of biodynamic feedthrough mitigation techniques. *IFAC Proceedings Volumes*, (pp. 316–321). Elsevier. 43.

Vrouwenvelder, S., Postema, F. M., & Pool, D. M. (2021). Measuring the drag latency of touchscreen displays for human-in-the-loop simulator experiments. In *Proceedings of the AIAA Modeling and Simulation Technologies Conference, Nashville (TN)*, Under review.

Watkins, C. B., Nilson, C., Taylor, S., Medin, K. B., Kuljanin, I., & Nguyen, H. B. (2018). Development of touchscreen displays for the Gulfstream G500 and G600 symmetryTM flight deck. *2018 IEEE/AIAA 37th Digital Avionics Systems Conference (DASC)*, (pp. 1–10). IEEE.

Zaal, P. M. T., Pool, D. M., Bruin, J. D., Mulder, M., & Van Paassen, M. M. (2009). Use of pitch and heave motion cues in a pitch control task. *Journal of Guidance, Control, and Dynamics*, *32*(2), 366–377. https://doi.org/10.2514/1.39953

## About the Authors

**Arwin Khoshnewiszadeh** received his B.Sc. (2016) and M.Sc. (2020) in Aerospace Engineering from TU Delft, The Netherlands. He has previously worked on modeling of Stewart platforms for maritime applications and software for Level-D flight simulators.

**Daan M. Pool** received his M.Sc. (2007) and Ph.D. (2012) degrees (*cum laude*) from TU Delft, The Netherlands. He is currently an Assistant Professor with the section Control and Simulation at the Aerospace Engineering faculty of TU Delft. His research interests include human performance modeling, manual control, and simulator-based training.